2216 *Biochemistry* **2010,** *49,* 2216–2226
DOI: 10.1021/bi9013038

BIOCHEMISTRY
including biophysical chemistry & molecular biology
Article

Signal Transducer and Activator of Transcription 6 (STAT6) Is a Novel Interactor of Annexin A2 in Prostate Cancer Cells

Susobhan Das, Praveenkumar Shetty, Mallika Valapala, Subhamoy Dasgupta, Zygmunt Gryczynski, and Jamboor K. Vishwanatha*

Department of Molecular Biology and Immunology and Institute for Cancer Research, University of North Texas Health Science Center, Fort Worth, Texas 76107

Received July 28, 2009; Revised Manuscript Received February 2, 2010

ABSTRACT: Annexin A2 (AnxA2) is a multifunctional Ca^{2+}-dependent phospholipid-binding protein, and its overexpression is implicated in malignant transformation of several cancers. In prostate cancer, however, the expression of AnxA2 is lost in prostate intraepithelial neoplasia and reappears in the high-grade tumors, suggesting a complex regulation of AnxA2 in the prostate microenvironment. Since a majority of the biological functions of AnxA2 are mediated by its interaction with other proteins, we performed a yeast two-hybrid assay to search for novel interactors of AnxA2. Our studies revealed that signal transducer and activator of transcription 6 (STAT6), a member of the STAT family of transcription factors, is a binding partner of AnxA2. We confirmed AnxA2−STAT6 interaction by in vitro co-immunoprecipitation and fluorescence resonance energy transfer (FRET) studies and demonstrated that AnxA2 interacts with phosphorylated STAT6. Furthermore, chromatin immunoprecipitation (ChIP) assay revealed that AnxA2 is associated with the STAT6 DNA-binding complex, and luciferase reporter assays demonstrated that AnxA2 upregulates the activity of STAT6. Upon interleukin-4 treatment, AnxA2 stabilizes the cytosolic levels of phosphorylated STAT6 and promotes its nuclear entry. These findings suggest that AnxA2−STAT6 interactions could have potential implications in prostate cancer progression. This report is the first to demonstrate the interaction of AnxA2 with STAT6 and suggests a possible mechanism by which AnxA2 contributes to the metastatic processes of prostate cancer.

Tumor cell invasion and metastasis are important prerequisites for tumor progression. Metastasis involves a series of coordinated and distinct steps that involve dissociation of single tumor cells from the site of the primary tumor, breakdown and invasion into the surrounding extracellular matrix (ECM), entry into the lymphatic or vascular space, and subsequent homing and proliferation in distant organs (*1*). Specific interactions of the tumor cells with the surrounding ECM and their ability to discharge from the barriers of the ECM are indispensable attributes of metastatically competent cells (*2*). Several proteases and their cell surface receptors have been shown to contribute to the malignant behavior of tumor cells characterized by their tendency to break down the ECM and metastasize to distant organs (*3*). Recent studies have indicated that dysregulation in the generation of plasmin contributes to the degradation of the ECM and facilitates the metastatic process (*4*). The generation of plasmin is regulated by specific cell surface receptors that could provide essential clues about the mechanism of tumor metastasis (*5*). Among the cell surface receptors for plasmin generation, AnxA2[1] is the best characterized and is known to facilitate an ~60-fold increase in the rate of generation of plasmin (*6*, *7*).

AnxA2 belongs to a family of multifunctional Ca^{2+}-dependent phospholipid-binding proteins that are expressed in various tissues and cell types (*8*). Cell surface-associated AnxA2 has been shown to bind to several components of the extracellular matrix (ECM) like tenascin C and several proteolytic components like procathepsin B, tissue plasminogen activator (tPA), and plasminogen (*9*−*11*). AnxA2-mediated plasmin generation facilitates the degradation of ECM and increases the invasive potential of several cancer cells, suggesting the direct involvement of AnxA2 in the malignant phenotype of tumor cells (*12*). Upregulation of AnxA2 expression has been reported to contribute to the malignant phenotype of breast (*13*), pancreatic (*14*), lung (*15*), kidney (*16*), and colorectal cancers (*17*) and is also associated with a poor clinical outcome (*18*), suggesting the oncogenic role of AnxA2. AnxA2 is suggested to be associated with prostate cancer metastasis (*19*, *20*), and other reports suggest that AnxA2 is downregulated in prostrate intraepithelial neoplasia (PIN) and is frequently re-expressed in high-grade prostate cancer (*21*, *22*). In addition, proteomic analysis has revealed that the expression of AnxA2 is lost or inhibited in prostate cancer cells in vivo and clinical prostate cancer specimens (*23*). Furthermore, re-expression of AnxA2 in metastatic prostate cancer cells inhibits the migration with no effects on cell proliferation or apoptosis (*23*). Although the mechanism by which loss of AnxA2 expression contributes to prostate cancer development is not known, the discrepancy in the expression levels of AnxA2 with the stage and grade of prostate cancer suggests a complexity in the regulation of AnxA2 expression in the prostate tumor microenvironment.

*To whom correspondence should be addressed: Graduate School of Biomedical Sciences, University of North Texas Health Science Center, 3500 Camp Bowie Blvd., Fort Worth, TX 76107. Phone: (817) 735-0224. Fax: (817) 735-0243. E-mail: jvishwan@hsc.unt.edu.

[1]Abbreviations: AnxA2, annexin A2; STAT6, signal transducer and activator of transcription 6; IL-4, interleukin-4; FRET, fluorescence resonance energy transfer; ChIP, chromatin immunoprecipitation; FLIM, fluorescence lifetime imaging microscopy.

 Published on Web 02/02/2010

In an effort to understand the molecular mechanisms associated with the regulation of AnxA2 expression in prostate cancer, we screened for the binding partners of AnxA2 using a yeast two-hybrid assay. We identified signal transducer and activator of transcription 6 (STAT6) as a binding partner of AnxA2.

Signal transducer and activator of transcription (STAT) proteins belong to a seven-member family of cytosolic proteins activated in response to cytokine and growth factor signaling with proposed functions as intracellular second messengers and transcription factors (*24*). In addition to their roles in normal cytokine signaling and development, members of the STAT family have been implicated in different pathological events like cellular transformation and oncogenesis (*25*). Several members of the STAT family, including STAT3 and STAT5, have been shown to contribute to the multistep process of tumor progression by activating several abnormal pathways of growth factor signaling which upregulate the invasive and metastatic potential of cancer cells (*26*−*28*). Previously, we have reported that STAT6 is constitutively activated in prostate cancer and functions as an important survival factor promoting the proliferation and migration of prostate cancer cells (*29*). STAT6 expression has been reported to be significantly upregulated in clinical tissue specimens compared to basal expression in normal tissues (*29*, *30*). In addition to its role in oncogenic transformation, defective STAT signaling also contributes to tumor progression as a result of the loss of immune surveillance (*31*).

The STAT signaling cascade involves binding of a cytokine to its cognate receptors, activation of the receptor-associated Janus kinases (JAKs), subsequent phosphorylation and activation of STAT proteins, dimerization followed by nuclear entry, and eventual transcription of STAT signature genes (*32*). Intracellular signaling of cytokines like IL-4 and IL-13 is known to be mediated through the STAT6 signaling pathway (*32*). Recent evidence indicates that IL-4 signaling mediated by STAT6 confers on cancer cells an improved invasive and metastatic ability (*30*, *33*). In addition, STAT6 deficient mice are shown to have a dramatically enhanced antitumor immunity against transplanted primary and metastatic tumors (*34*, *35*). IL-4 signaling mediated by STAT6 is also shown to have a potential role in the progression of androgen-independent prostate cancer (*36*). Although these reports suggest the importance of STAT6 signaling in the pathophysiology of prostate cancer, the exact mechanism involved in STAT6-mediated oncogenic responses is not known.

In this study, we propose a novel role of STAT6 as a binding partner of AnxA2. In addition to the yeast two-hybrid assay, we confirmed the interaction by immunoprecipitation and also demonstrated that AnxA2 enhances the transcriptional activity of STAT6 by its interaction with the STAT6 transcriptional complex. Taken together, our results suggest that AnxA2−STAT6 interactions could have potential implications in prostate cancer progression.

EXPERIMENTAL PROCEDURES

Cell Culture and Transfections. LNCaP, PC-3, DU-145, HeLa, and HPV 18-C1 cells were grown and maintained as previously reported (*22*, *37*). LNCaP-derived stable cell lines (ANX-3, C1-2, LNCaP-12/13-expressing ectopic, and tetracycline regulatable AnxA2) were maintained in complete RPMI 1640 medium containing 7% fetal bovine serum (FBS), 100 IU/mL penicillin, and 100 μg/mL streptomycin (GIBCO). Transfection of cells was performed using the Lipofectamine 2000 transfection reagent (Invitrogen Corp., Carlsbad, CA) following the manufacturer's instructions.

Yeast Two-Hybrid Screening. The full-length human AnxA2 cDNA (GenBank entry NM_004039) fragment was cloned into vector pGBKT7 (Clontech). The recombinant plasmid was used as a GAL4 DNA binding bait (DNA-BD/bait) and transformed into AH109 yeast cells that were screened for growth on synthetic dropout (SD/−Trp) medium. A human placental pretransformed cDNA library (Clontech) was used for screening interacting proteins. This library was made in vector pGADT7-rec that contains the activation domain (DNA-Ac/library) with a different nutrient marker −Leu and was transformed into strain Y187 and screened for growth on SD/−Leu medium. The interaction screening was conducted by mating the DNA-BD/bait strain and DNA-Ac/library strain, and the positive clones were selected according to the manufacturer's instructions (Clontech). Positive clones were selected on high-stringency medium with selection markers SD/−Ade/−His/−Leu/−Trp/X-α-gal and then screened as described above (Clontech). Positive yeast clones were selected by prototrophy for histidine or expression of β-galactosidase and then subjected to sequence analysis to search for novel AnxA2 binding proteins.

Generation of AnxA2-Expressing Stable LNCaP Cells. Full-length AnxA2 cDNA was cloned as a BamHI−NheI fragment into doxycycline-inducible vector pBIG2i (gift from J. Reeder, University of Rochester, Rochester, NY). The stable cells were selected by being cultured in the presence of 500 μg/mL hygromycin B (Boehringer Mannheim GmbH, Mannheim, Germany). After individual colonies had been selected, the expression levels of AnxA2 were assessed by Western immunoblot and immunocytochemistry. One of the individual clones, LNCaP-12, was used in subsequent experiments.

To generate a LNCaP cell line stably expressing the AnxA2−GFP fusion protein, we cloned AnxA2 cDNA as a BamHI−NheI fragment into vector pEGFP-C1 (Clontech). The stable clones were selected by being cultured in the presence of 0.5 mg/mL G418 (Sigma, St. Louis, MO), and one of the clones was named ANX-3. Similarly, stable clones expressing the pEGFP-C1 empty vector were established and named LNCaP C1-2. The cell lines were tested for AnxA2 and GFP expression by Western immunoblotting.

Generation of Luciferase Reporter Constructs. LNCaP, LNCaP-12, ANX-3, C1-2, DU-145, and PC-3 cell lines were used for the luciferase assay using translucent reporter vectors for STAT6 and a nontargeting translucent vector (Interchim Inc.). To normalize for the activity of the experimental reporter and to reduce experimental variability, we made use of a dual-luciferase assay system (Promega, Madison, WI).

The luciferase reporter construct (2 μg) was cotransfected along with 400 ng of *Renilla* luciferase plasmid construct (pRL-SV40, gift from M. Kim, University of North Texas Health Science Center). AnxA2 expression was induced using 2 μg/mL doxycycline. After being incubated for 48 h, the cells were lysed, and luciferase activity measured in a TD 20/20 luminometer (Turner Biosystems) using the dual luciferase reporter assay kit (Promega). Relative luciferase activity was obtained by determining the ratios of reporter luciferase versus *Renilla* luciferase activities. Statistical analysis of the data was conducted using a one-way ANOVA from at least three independent transfection experiments.

Cloning and Expression of Recombinant AnxA2. Full-length AnxA2 cDNA was cloned as a BamHI−XhoI fragment into GST vector pGEX-5X-3 (Amersham Biosciences, GE Healthcare Bio-Sciences Corp., Piscataway, NJ) and transformed into BL-21 competent cells for recombinant GST−AnxA2 protein expression. The fusion protein was induced to be expressed in the presence of isopropyl D-thio-galactopyranoside (IPTG) (Promega), and sequence integrity was confirmed by sequence analysis of the plasmid DNA. Expression of the GST−AnxA2 fusion protein was confirmed by Western blot analysis using both the anti-GST monoclonal antibody (Santa Cruz Biotechnology, Santa Cruz, CA) and the anti-AnxA2 monoclonal antibody (BD Biosciences, San Jose, CA).

Immunoprecipitation. Whole cell lysates from DU-145 and PC-3 cells were subjected to immunoprecipitation with anti-AnxA2 and anti-STAT6 antibodies using the commercially available protein A/G-coated immunoprecipitation plate kit (Pierce, Rockford, IL) following the manufacturer's instructions. Immunoprecipitation was also performed using the GST−AnxA2 fusion protein and recombinant STAT6 with anti-AnxA2 and anti-STAT6 antibodies (BD Biosciences).

Cell Fractionation and Immunoblotting. Cell fractionation and Western immunoblotting were performed as previously described (*37*). The purity of nuclear and cytosolic extracts was determined by immunoblotting with lamin and GAPDH antibodies, respectively.

Cell-Based ELISA. A cell-based ELISA was performed to analyze the pSTAT6 level in AnxA2-null LNCaP cells and ANX-3 cells. In brief, cells were cultured in 96-well plates and treated with IL-4 (20 ng/mL) for 20 min. The cells were fixed, and the extent of STAT6 phoshorylation on tyrosine 641 was determined using a pSTAT6 (Y-641) cell-based ELISA kit (R&D Systems Inc., Minneapolis, MN) according to the manufacturer's instructions.

RNAi-Mediated Silencing of AnxA2 Expression and Luciferase Reporter Assay. DU-145 and PC-3 cells were transfected with 100 nM AnxA2 SiRNA (Dharmacon, Lafayette, CO) as previously published (*38*). The levels of STAT6 transcription upon AnxA2 silencing were determined via cotransfection of STAT6 luciferase reporter or control constructs 24 h after AnxA2 siRNA transfection as described previously.

Determination of the Förster Distance (R_0) for Alexa Fluor 488 and 594-Labeled Proteins. The Förster radius (R_0) is the distance between the donor and acceptor that would enable 50% energy transfer. The R_0 value was determined by analyzing the fluorescence spectra of the donor and the donor−acceptor pair to determine the overlap integral $J_{(\lambda)}$, which is a measure of the spectral overlap between the donor emission and acceptor absorption and is calculated from the formula

$$J(\lambda) = \frac{\int_0^\infty F_D(\lambda)\varepsilon(\lambda)\lambda^4 \, d\lambda}{\int_0^\infty F_D(\lambda) \, d\lambda}$$

where $F_D(\lambda)$ is the fluorescence emission of the donor in the wavelength ranging form of λ to $\lambda + \Delta\lambda$ obtained after normalization of the area under the curve, $\varepsilon(\lambda)$ is the extinction coefficient of the acceptor at λ expressed in units of M^{-1} cm^{-1}, and λ is the wavelength in nanometers (*35*). $J(\lambda)$ is represented in units of M^{-1} cm^{-1} nm^4.

The R_0 value which is the characteristic Förster distance is calculated from the equation

$$R_0 = 9.78 \times 10^3 [k^2 n^{-4} Q_D J_{(\lambda)}]^{1/6}$$

where k^2 is the dipole−dipole coupling factor, n is the refractive index of the medium, and Q_D is the quantum yield of the donor. Using this equation, R_0 is calculated to be 43 Å for the Alexa Fluor 488 and Alexa Fluor 594 fluorophores.

Fluorescence Lifetime Imaging Microscopy (FLIM) and Förster Resonance Energy Transfer (FRET) Imaging of Alexa-Labeled AnxA2 and STAT6 Interactions. PC-3 cell lines were seeded on the glass coverslips, and immunocytochemistry was performed with anti-AnxA2 (0.2 μg/mL, BD Biosciences) and anti-STAT6 (0.8 μg/mL, BD Biosciences) as previously described (*37*). AnxA2 and STAT6 were labeled with Alexa Flour 488 and Alexa Flour 594 secondary antibodies, respectively. To determine the FRET efficiency and measure the physical distance between the two fluorophores, steady state fluorescence lifetimes of the donor and the donor−acceptor pair were measured using fluorescence lifetime imaging microscopy (FLIM) using the custom equipped MicoTime 200 single-photon counting microscopy system (PicoQuant GmbH). For our experiments, we used a 470 nm pulsed laser diode (20 MHz repetition rate) as the excitation source and a Perkin-Elmer detector. The images were taken using an OLYMPUS 60× water immersion objective (NA 1.2). The excitation pulse width at the sample place was below 100 ps, and the time response of the Perkin-Elmer detector has been estimated to be ~300 ps. Time-resolved fluorescence decays of the donor and the donor−acceptor pair were analyzed using the method previously published (*39*, *40*). The efficiency of energy transfer was obtained from the fluorescence lifetimes of the donor using the formula $E = 1 - \tau_{DA}/\tau_D$, where τ_D and τ_{DA} are the fluorescence lifetimes of the donor and donor−acceptor pair, respectively. The FRET distances between the donor and donor−acceptor pair were calculated using the energy of efficiency (E) and R_0 values obtained from the previous equations using the formula $R = R_0[(1 - E)/E]^{1/6}$, where R is the physical distance (angstroms) between the fluorophore-tagged proteins, R_0 is the Förster distance, and E is the efficiency of energy transfer.

Chromatin Immunoprecipitation (ChIP) Assay. The ChIP assay was performed on DU-145 cells as described previously (*41*). Briefly, DU-145 cells were cross-linked with 1% paraformaldehyde for 10 min, lysed, and sonicated to shear the chromosomal DNA. The supernatant was collected after centrifugation and incubated with protein A/G beads (Sigma) at 4 °C, and immunoprecipitation was performed with anti-STAT6 antibody overnight at 4 °C. Half of the immunoprecipitates collected were subjected to Western immunoblot analysis, and the other half were used for PCR analysis. DNA was purified and analyzed by PCR using the following primers for the IgE promoter (5′−3′): forward, TGG GCC TGA GAG AGA AGA GA; reverse, AGC TCT GCC TCA GTG CTT TC (yielding a product of 174 bp).

Electrophoretic Mobility Gel Shift Assay (EMSA). STAT6 DNA binding activity was determined by gel shift assays using the STAT6 specific EMSA gel shift kits (Panomics Inc., Redwood City, CA). Nuclear extracts from LNCaP, PC-3, DU-145, and LNCaP-12 cells untreated and treated with (2 μg/mL) doxycycline were used. The assay was performed as previously described (*42*).

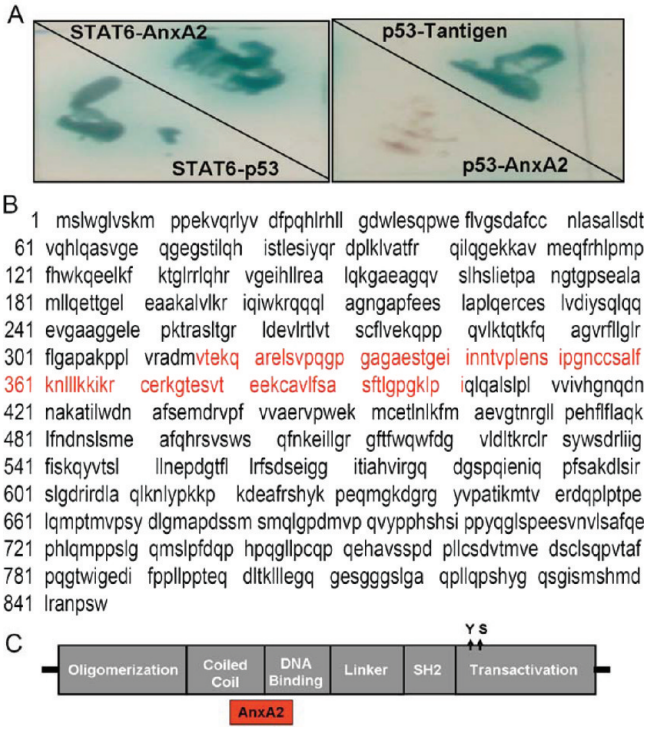

FIGURE 1: STAT6 interacts with AnxA2 in a yeast two-hybrid screen. (A) Positive clones were selected on high-stringency medium (synthetic dropout medium) selection markers SD/−Ade/−His/−Leu/−Trp/X-α-gal, and only true interactors can activate the expression of β-galactosidase (blue color). The left panel shows positive interaction of STAT6 with AnxA2, and p53. The right panel shows the positive control p53−T-antigen interaction, while the AnxA2−p53 interaction served as the negative control. (B) Sequence analysis of the positive putative interactor of STAT6 clones confirmed a stretch of 85 amino acids in STAT6 protein, as indicated by the red color. (C) Cartoon showing that the AnxA2 interacting domain of STAT6 lies between the coiled-coil and DNA-binding domains of the STAT6 protein.

RESULTS

STAT6 Is a Novel Interacting Protein of AnxA2. Full-length AnxA2 cDNA cloned into the GAL4 DNA-binding domain (GAL4 DNA-BD) of vector pGBKT7 was used as a bait plasmid to screen for interacting proteins from a randomly primed and pretransformed human placental cDNA library fused to the GAL4 activation domain (pGADT7-rec-cDNA). Figure 1A (left panel) shows the blue colonies representing the interaction between AnxA2 and STAT6 and a positive interaction of STAT6 and p53. In both cases, the intensity of the blue color matches that of the known positive control (p53 and T-antigen) compared to the negative control (p53-AnxA2) that shows minimal growth and color development (Figure 1A, right panel). After screening for true positive blue colonies, we used isolated pGADT7-plasmid DNA to transform Y187 cells, and we repeated the screening assay to reconfirm the interaction. True positive clones were selected, and DNA sequencing revealed 12 different genes, of which three clones appeared to be of the STAT6 cDNA sequence. Sequence analysis showed that the STAT6 clones contained an open reading frame (ORF) of 85 amino acids (indicated by the red bar in Figure 1C) and a poly(A) tail. The sequences were identical in all three clones representing STAT6, and a BLAST search indicated that the ORF has homology with the STAT6 gene (GenBank entry NM_003153) in the region of amino acids 316−401 (GenBank entry NP_003144) (Figure 1B). A schematic representation of the domains of STAT6 and the putative site of interaction that spans the coiled-coil and DNA-binding domains of STAT6 is shown in Figure 1C.

To validate AnxA2−STAT6 interaction in cancer cells, we performed immunoprecipitation for AnxA2 and STAT6 in DU-145 and PC-3 prostate cancer cells. The cell lysates were immunoprecipitated with anti-AnxA2 antibody and immunoblotted with anti-STAT6 antibody to determine if STAT6 can be coprecipitated with AnxA2. A 100 kDa band corresponding to the molecular mass of STAT6 was detected in both DU-145 and PC-3 immunoprecipitates (Figure 2A). Reverse immunoprecipitation with anti-STAT6 antibody and immunoblotting with anti-AnxA2 antibody also revealed AnxA2 as a coprecipitant (Figure 2B). In view of the abundance of AnxA2 in DU-145 and PC-3 cells, the relative intensity of the AnxA2 band is significantly higher than that of the STAT6 band. However, both IP and reverse IP using different antibodies show interaction of STAT6 and AnxA2. Since phosphorylation of STAT6 is known to be associated with its downstream signaling (*43*), we wanted to determine if AnxA2 interacts with the phosphorylated and/or unphosphorylated STAT6. For this, we immunoprecipitated AnxA2 from DU-145 and PC-3 lysates using anti-AnxA2 antibody and probed for phosphoSTAT6. Our results clearly show that phosphorylated STAT6 is indeed a binding partner of AnxA2 in both DU-145 and PC-3 lysates compared to nonspecific IgG controls (Figure 2C).

To demonstrate AnxA2 has a binding affinity for STAT6 in vitro, we incubated recombinant GST−AnxA2 fusion protein and STAT6 (rSTAT6) either in the presence or in the absence of calcium, followed by immunoprecipitation to recover the interactor complex. Since AnxA2 is a Ca^{2+}-binding protein and it is known that many of the interactions of AnxA2 are influenced by intracellular levels of Ca^{2+} (*44*, *45*), we examined if Ca^{2+} has any role in the AnxA2−STAT6 interaction. As shown in Figure 2D, STAT6 was immunoprecipitated with anti-GST antibody, suggesting a strong interaction between AnxA2 and STAT6. However, the interaction was not found to be influenced by calcium levels by addition of $CaCl_2$ or chelation of Ca^{2+} by EGTA. Interestingly, a second band was observed at 110 kDa which represents the truncated form of STAT6. Immunoprecipitation with nonspecific mouse IgG did not yield the corresponding band of STAT6.

Fluorescence Lifetime Imaging Microscopy (FLIM) Confirms the Interaction of STAT6 and AnxA2. To determine the AnxA2−STAT6 complex exists as a close complex in the physiological state, we performed fluorescence lifetime imaging microscopy (FLIM)-based fluorescence resonance energy transfer (FRET) assays in PC-3 cells. Typically, FRET occurs when two proteins are no more than 8−10 nm apart. To calculate FRET, PC-3 cells were treated with AnxA2 and STAT6 antibodies (primary) followed by Alexa-conjugated (secondary) antibodies labeled with fluorophores 488 and 594 nm detecting AnxA2 and STAT6, respectively. To detect the fluorescence energy transfer, PC-3 cells labeled with AnxA2-488 served as a donor whereas STAT6-594 as an acceptor, and lifetime measurements were calculated between the donor and the donor−acceptor pair. Fluorescence lifetime decay of the donor was measured to be 2.75 ns, and the decay for the donor−acceptor pair was measured to be 2.35 ns; these value are represented in false color images and the lifetime histograms of both the donor and the donor−acceptor pair (Figure 3A,B). Intensity-averaged

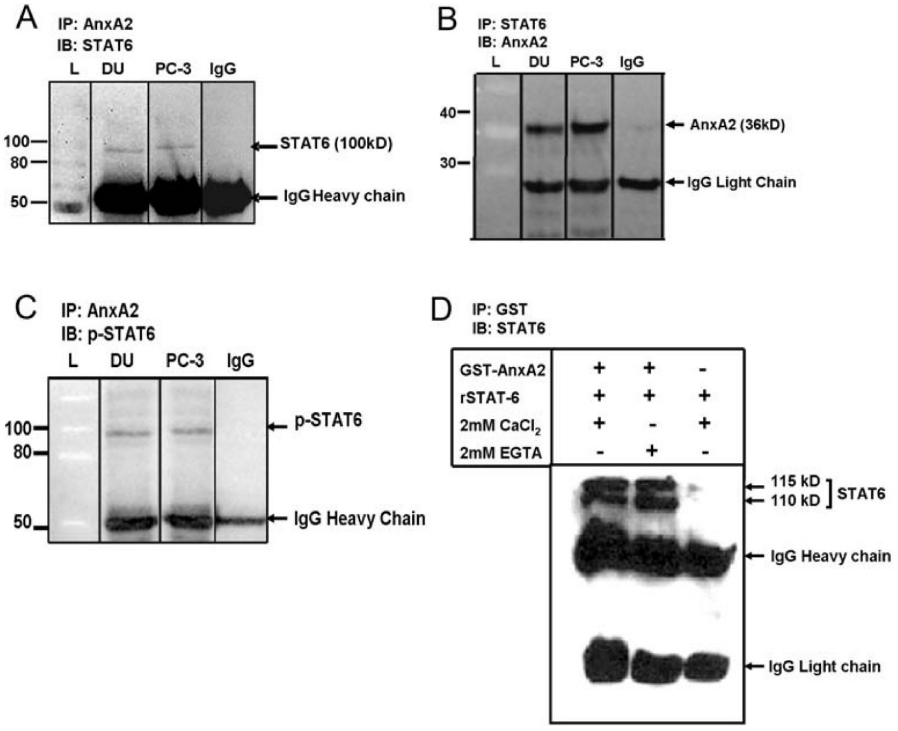

FIGURE 2: Pull-down assays show STAT6 as an interactor of AnxA2. DU-145 and PC-3 whole cell lysates were (A) immunoprecipitated with AnxA2 or IgG (control) antibody and immunoblotted with STAT6 antibody, (B) immunoprecipitated with STAT6 or IgG (control) antibody and immunoblotted with AnxA2 antibody, and (C) immunoprecipitated with AnxA2 or IgG (control) antibody and immunoblotted with p-STAT6 antibody. (D) GST−AnxA2 fusion protein and recombinant STAT6 (rSTAT6) were preincubated in the presence of $CaCl_2$ or EGTA, and protein complexes were then pulled down with GST antibody and blotted with STAT6 antibody. L indicates the protein ladder used in SDS−PAGE. IP, immunoprecipitation; IB, immunoblotting.

lifetimes of the donor (blue) and donor−acceptor pair (red) were fitted to a distribution curve (black) as shown in Figure 3C. Substituting the lifetime values in the Förster equation, we determined the efficiency of energy transfer to be 30% which in turn corresponds to a distance of 49 Å between the donor and acceptor pair. These results clearly demonstrate that there is a strong interaction between AnxA2 and STAT6 in PC-3 cells.

Chromatin Immunoprecipitation (*ChIP*) *of AnxA2 Yields a STAT6 Specific Promoter*. Since STAT6 is a transcription factor and its interaction with its cognate DNA binding sites is known to be influenced by interaction with several activator proteins (*46*), we wanted to determine if AnxA2 is associated with STAT6 interacting elements in the DNA. To confirm that AnxA2 is a part of the STAT6 DNA-binding complex, a ChIP assay was performed on DU-145 cells. Following formaldehyde cross-linking to stabilize the interactions and sonication to shear DNA, we subjected the extracts to immunoprecipitation and PCR analysis. Immunoprecipitation of the DNA−protein complexes with anti-AnxA2 antibody showed a strong band corresponding to STAT6 compared to a negative control IgG antibody, and the intensity of the STA6 band was proportional to the amount of protein loaded on the gel (Figure 4A). PCR analysis with primers specific for the IgE promoter, a downstream target of STAT6, demonstrated the presence of a 174 bp product in the ChIP extracts immunoprecipitated with anti-AnxA2 antibody which was absent in the extracts immunoprecipitated with nonspecific anti-mouse IgG antibody (Figure 4B).

AnxA2 Potentiates IL-4-Mediated Phosphorylation of STAT6. The STAT family of proteins is known to be activated by phosphorylation in response to extracellular signaling mediated by cytokine, growth factor, and hormone signaling (*24*). In normal cells, the activation of STAT is a transient and highly regulated process (*47*). In cancer cells, however, STATs are constitutively activated and known to play important roles in several malignancies (*25*). Binding of IL-4 and the activation of the IL-4 receptor result in the phosphorylation of STAT6 at Y641 by IL-4 receptor-associated Jak kinases (*48*). Phosphorylation of STAT6 at Y641 is known to be essential for its dimerization and nuclear entry (*32*). Since our studies have indicated that AnxA2 is a binding partner of STAT6, we wanted to determine if binding of AnxA2 to STAT6 influences its phosphorylation status and nuclear entry. For this purpose, we treated ANX-3 and LNCaP cells with 20 ng/mL IL-4 and analyzed the phosphorylation of STAT6. On IL-4 treatment, an increase in the cytosolic and nuclear levels of phosphorylated STAT6 was observed in ANX-3 cells constitutively expressing AnxA2. In the AnxA2 null LNCaP cells, however, IL-4 treatment did not result in an induction in the cytosolic or nuclear levels of phosphorylated STAT6. In both ANX-3 and LNCaP cells, basal levels of phosphorylated STAT6 were observed in cells that were not treated with IL-4. These results suggest that AnxA2 facilitates the IL-4-mediated phosphorylation of STAT6. The cytosolic levels of unphosphorylated STAT6 remained invariant in both ANX-3 and LNCaP cells and were not influenced by IL-4 stimulation. The purity of nuclear and cytosolic extracts was confirmed by immunoblotting with lamin and GAPDH, respectively (Figure 5A).

To further demonstrate that AnxA2 influences the phosphorylation and nuclear entry of STAT6, we performed a cell-based ELISA on IL-4-stimulated and unstimulated LNCaP and ANX-3 cells. We observed a significant increase in the levels of phosphorylated STAT6 in both unstimulated and IL-4-stimulated ANX-3 cells compared to the LNCaP cells (Figure 5B).

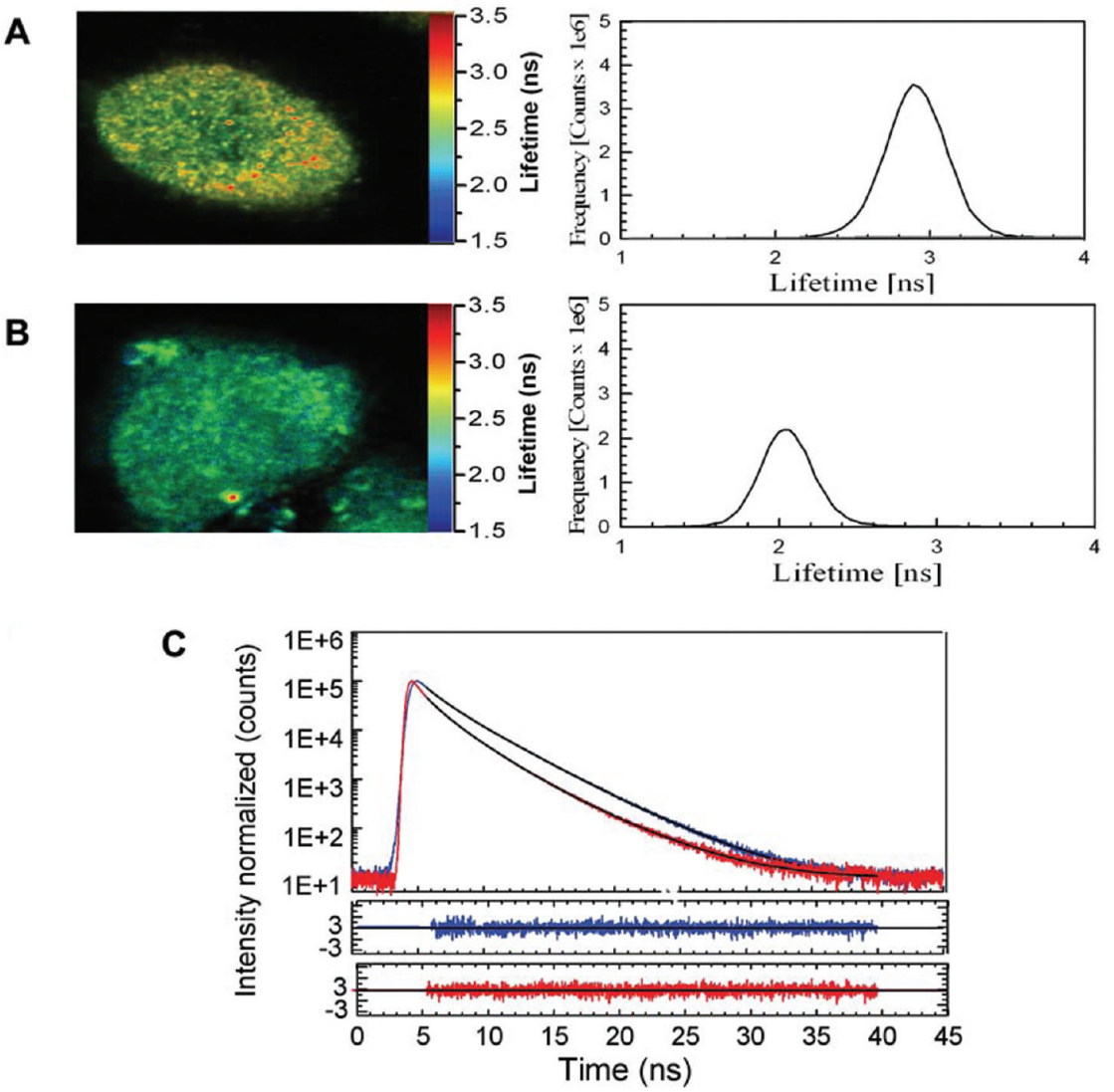

FIGURE 3: Fluorescence lifetime imaging microscopy confirms the interaction of STAT6 and AnxA2. Lifetime decays of the donor and donor−acceptor pair were measured to be 2.72 and 2.35 ns, respectively, and are represented in false color images and lifetime decay histograms of the donor (A) and donor−acceptor pair (B). Panel C shows intensity-averaged lifetimes of the AnxA2 donor (blue) (2.72 ns) as compared to AnxA2−STAT6 interaction donor−acceptor pair (red) (2.35 ns). Putting these values into Förster's equation, we obtain an efficiency of energy transfer (E = 30%) and a molecular distance (r = 49 Å).

These results suggest that AnxA2 is involved in the phosphorylation and nuclear translocation of STAT6 and could have a potential role in the STAT6-mediated IL-4 downstream signaling events.

Binding of AnxA2 to STAT6 Enhances the Transcriptional Activity of STAT6. Our previous results have indicated that AnxA2 increases the cytosolic and nuclear levels of phosphorylated STAT6 on IL-4 stimulation. Next, we wanted to determine if AnxA2 could enhance STAT6 transcriptional activity. To demonstrate this, we performed a dual luciferase reporter assay with a construct containing a STAT6 enhancer element fused upstream to a luciferase reporter and a control construct containing a nonspecific enhancer element cloned upstream of the luciferase. The assay was performed with AnxA2 null LNCaP cells and LNCaP-12 cells expressing tet-inducible AnxA2. Upon transfection with the STAT6 luciferase reporter construct or a control construct along with a *Renilla* luciferase vector, luciferase activities were measured. As shown in Figure 6A, a significant (10-fold) increase in the relative luciferase activity of the luciferase reporter compared to that of *Renilla* luciferase was observed in the LNCaP-12 cells on induction with doxycycline compared to the LNCaP-12 cells transfected with the control vector. Parental LNCaP cells, however, exhibited basal luciferase activity when transfected with both the reporter and control constructs. In addition, Western immunoblot analysis also demonstrated an increase in the level of expression of AnxA2 in LNCaP-12 cells in the presence of doxycycline compared to that of the uninduced cells (Figure 6B).

We further demonstrated the effects of AnxA2 overexpression on the transcriptional activity of STAT6 in ANX-3 cells with constitutive overexpression of AnxA2 and LNCaP C1-2 cells stably transfected with the pEGFP-C1 empty vector. Relative luciferase activity was represented as a ratio of the luciferase activity of the luciferase reporter and the *Renilla* plasmid. We observed an ~10-fold increase in the relative luciferase activity in ANX-3 cells compared to LNCaP C1-2 cells (Figure 6C). Cells transfected with the reporter construct, however, exhibited no significant luciferase activity. These results conclude that overexpression of AnxA2 not only increases the cytosolic and nuclear levels of phosphorylated STAT6 but also promotes the transcriptional activity of STAT6.

siRNA-Mediated Downregulation of AnxA2 Decreases STAT6 Transcriptional Activity. Since overexpression of AnxA2 results in an upregulation of STAT6 transcriptional activity, we examined the effect of downregulation of AnxA2 on STAT6 transcriptional activity. AnxA2 siRNA was used to downregulate the expression of AnxA2 in DU-145 and PC-3 cell lines, and the transcriptional activity of STAT6 was measured using a luciferase reporter assay. As shown in Figure 7A, a significant decrease in luciferase activity in both cell lines was observed upon downregulation of AnxA2 with specific siRNA compared to the luciferase activity in cells transfected with a control luciferase construct. The effect of AnxA2 siRNA in downregulating the expression of AnxA2 was tested by Western immunoblot analysis of protein lysates from DU-145 and PC-3 cells. As shown in Figure 7B, AnxA2 siRNA resulted in an ~80−90% reduction in the expression levels of AnxA2 in both DU-145 and PC-3 cells. These results provide further proof for our previous observations that AnxA2 upregulates the transcriptional activity of STAT6 and suggest that AnxA2 could have potential implications in the STAT6-mediated signaling pathways.

AnxA2 Stimulates STAT6 DNA Binding Activity in Prostate Cancer Cells. Since our data indicate that AnxA2 influences the transcriptional activity of STAT6, we wanted to determine if AnxA2 affects the STAT6 DNA binding activity. An electrophoretic mobility shift assay (EMSA) clearly shows STAT6 DNA binding activity in the nuclear extracts of DU-145 cells, and the STAT6 band was further supershifted in the presence of STAT6 (*) and AnxA2 (^) antibody, indicating the presence of the STAT6−AnxA2 complex in the nuclear lysates (Figure 8A). Furthermore, the STAT6 DNA binding activity was increased in LNCaP-12 cells (expressing *tet*-inducible AnxA2) treated with doxycycline, compared to untreated cells, validating the fact that AnxA2 expression and binding with its partner molecule STAT6 significantly upregulate STAT6 DNA binding activity. As a control, HeLa cells nuclear extract was incubated with STAT6 probe in the presence of doxycycline (Figure 8B, lane 4).

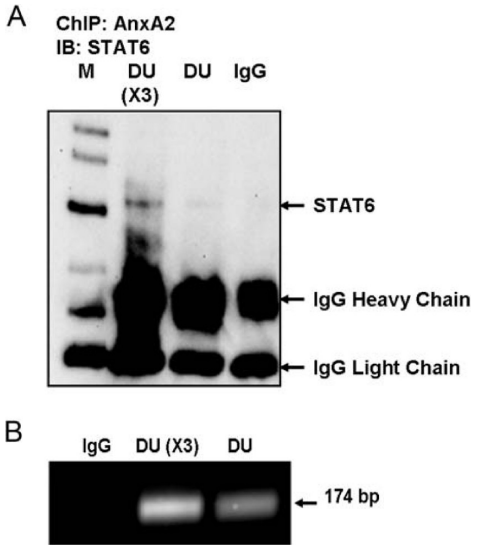

FIGURE 4: Chromatin immunoprecipitation using AnxA2 antibody yields the promoter for IgE. The ChIP showed both the presence of STAT6 in Western blot analysis (A) and the presence of the IgE promoter, a known STAT6 DNA target via PCR (B). ×3 for each panel denotes triple the amount of protein and RNA loaded.

DISCUSSION

Overexpression of AnxA2 is associated with progression and metastasis of several cancers and is correlated with a high nuclear grade of the tumor and poor clinical outcome (*12*, *49*). On the other hand, AnxA2 expression is downregulated in the initial progression of prostate cancer and reexpression occurs in the later stages of prostate carcinoma (*21*, *22*). This discrepancy is attributed to the differences in the putative functions of AnxA2 in specific histological microenvironments (*23*). To improve our understanding of the role of AnxA2 in the progression of prostate cancer, we wanted to investigate the novel binding partners of AnxA2.

In this study, we employed a yeast two-hybrid assay to identify novel interactors of AnxA2. Of the 13 positive clones obtained in the study, we found STAT6 to be a novel interactor of AnxA2 in three independent clones. The interaction was also confirmed in vitro and in vivo by co-immunoprecipitation and also by FRET studies. Since AnxA2 is a Ca^{2+}-binding protein, its interaction with other proteins is influenced by the cellular levels of Ca^{2+} (*45*). Immunoprecipitation of the AnxA2−STAT6 complex in the presence of $CaCl_2$ and EGTA indicated that AnxA2−STAT6 interaction is not influenced by cellular levels of Ca^{2+},

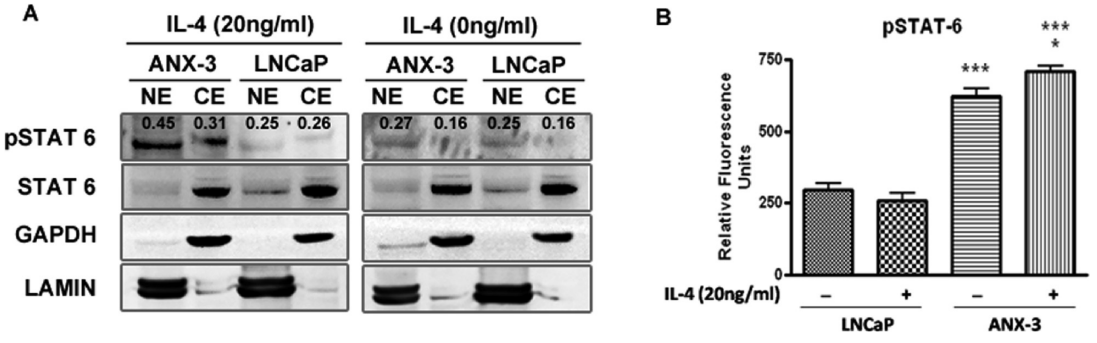

FIGURE 5: AnxA2 increases the extent of phosphorylation and nuclear translocation of STAT6 in prostate cancer cells. (A) LNCaP and ANX-3 cells were either unstimulated or stimulated with IL-4 (20 ng/mL) for 20 min. Cytosolic and nuclear extracts (40 μg) were separated on a 4−12% Bis-Tris gel and blotted with specific antibodies. The numerical values in the first panel represent pSTAT6/STAT6 optical density readings after normalization with respective loading controls. The figure shown is a representative of the three individual experiments. (B) AnxA2 induces STAT6 phosphorylation in LNCaP cells. LNCaP and ANX-3 cells were cultured in 96-well plates and treated with 20 ng/mL recombinant human IL-4 for 20 min. Levels of phosphoSTAT6 (on Y641) were determined using a cell-based ELISA. Results are representative of multiple experiments, each performed with duplicate samples. One asterisk indicates $p < 0.05$ (with or without IL4 in Anx-3 cells), and three asterisks indicate $p < 0.001$ (with two different cell lines).

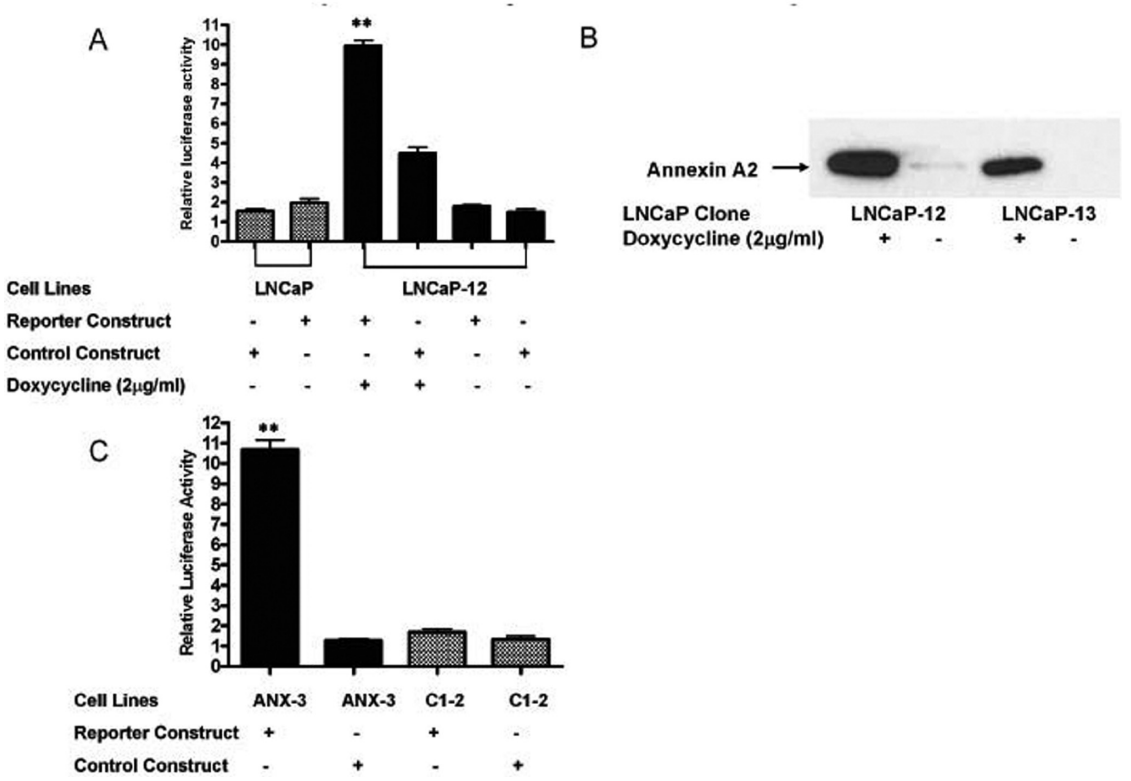

FIGURE 6: AnxA2 stimulates STAT6 transcriptional activity by interacting with STAT6. (A) A luciferase reporter construct was transiently transfected into LNCaP and LNCaP-12 cells as described in Experimental Procedures. For control experiments, the construct with the nonspecific enhancer sequence was used. *Renilla* luciferase constructs (400 ng of plasmid DNA) were cotransfected with either reporter or control constructs in all experiments. Doxycycline (2 μg/mL) was added 24 h post-transfection to induce AnxA2 protein expression followed by analysis of cell extracts for luciferase activity. The relative luciferase activity is presented as a percentage of activity obtained as a ratio of luciferase reporter activity to that of *Renilla* luciferase activity. Each column and bar represents the mean ± standard error from three independent transfections. (B) Western blot to show the tight regulation of AnxA2 protein expression from the doxycycline-inducible construct stably transfected into LNCaP clones. Anti-AnxA2 monoclonal antibody (BD Biosciences) was used at dilution of 0.4 μg/mL. (C) Luciferase assay performed in ANX-3 and C1-2 cells that stably express GFP-fused AnxA2 and only GFP proteins, respectively. The assay was performed as described above and relative luciferase activity reported.

suggesting the involvement of AnxA2 in Ca^{2+}-independent processes.

Structurally, STAT6 contains six distinct domains that are structurally and functionally conserved among the STAT family (*50*). They include the N-terminal oligomerization domain that is necessary for stabilizing the interactions among other DNA-bound STAT proteins, a coiled-coil domain that is necessary for protein−protein interactions, a DNA-binding domain, an EF-hand-like linker domain connecting the DNA-binding and SH2 domain, SH2 domain necessary for phosphorylation-regulated activities, and a C-terminal transactivation domain (*24*). In our studies, DNA sequence analysis of the three clones of STAT6 revealed that the region comprising the coiled-coil and DNA-binding domain of STAT6 is involved in the interaction with AnxA2. The presence of a putative AnxA2-binding site spanning the DNA-binding domain of STAT6 suggests a potential role of AnxA2 in mediating the DNA binding activities of STAT6.

Cytokine signaling through STAT6 involves a series of regulatory steps that are initiated by the binding and activation of the cytokine receptor, recruitment of JAKs, and binding of STAT6 to tyrosine-phosphorylated residues in the cytokine receptor, activation of STAT6 by phosphorylation at tyrosine 641, dimerization, and translocation to the nucleus (*24*). In our studies, we observed that AnxA2 co-immunoprecipitates with phosphorylated STAT6. In addition, AnxA2 was also immunoprecipitated with STAT6 DNA-binding elements, suggesting that AnxA2 could have potential roles in regulating the functions of phosphorylated STAT6.

Since STAT6 does not possess a nuclear localization signal (NLS) and nuclear translocation of phosphorylated STAT6 is important for its transcriptional activity (*51*), it is essential to identify new molecular mediators involved in this process. Previous studies have indicated the association of STAT6 with a detergent-sensitive chaperone-like molecule that could stabilize the phosphorylated STAT6 dimers in the cytosol by binding to and masking the DNA-binding domain (*51*). On translocation to the nucleus, the chaperone is released, enabling the activated STAT6 to bind to its cognate elements on the DNA (*51*). Further studies are needed to ascertain whether AnxA2 acts a chaperone to stabilize the phosphorylated STAT6 in the cytosol and also facilitate the nuclear entry and DNA binding activity of phosphorylated STAT6.

Our results also suggest that upon IL-4 treatment, nuclear and cytosolic levels of phosphorylated STAT6 were significantly increased in ANX-3 cells overexpressing AnxA2 compared to AnxA2 null LNCaP cells. These results suggest that AnxA2 potentiates IL-4-induced phosphorylation of STAT6 by a yet unidentified mechanism. Interestingly, we also observed a dramatic increase in the STAT6 DNA binding activity and a concomitant increase in the STAT6 transcriptional activity in cell lines overexpressing AnxA2. Also, the transcriptional activity

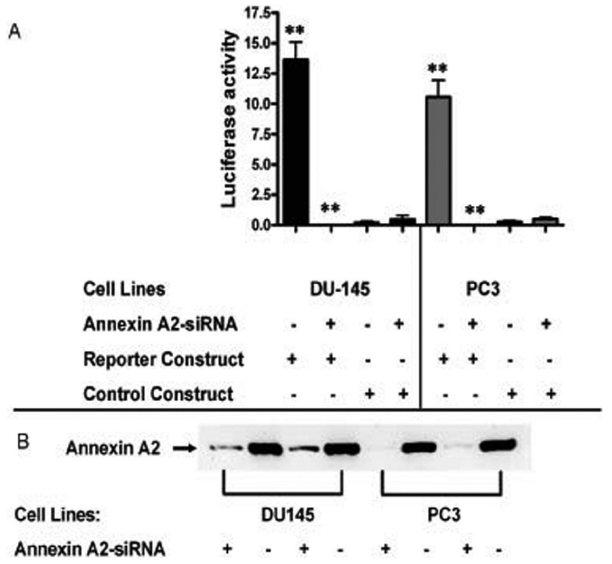

FIGURE 7: siRNA-mediated downregulation of AnxA2 decreases STAT6 transcriptional activity. (A) Luciferase assays were performed in DU-145 and PC-3 cells with or without downregulation of AnxA2 gene expression by using AnxA2 specific siRNA. AnxA2 siRNA was transfected to the cells after primary transfection with luciferase constructs for 24 h. In this particular assay, *Renilla* luciferase activity was not included to prevent excessive cytotoxicity from the transfection reagent. Each column and bar represents the mean ± standard error from three independent experiments. (B) Western blot analysis of siRNA-treated and untreated samples to show the levels of downregulation of AnxA2 in DU-145 and PC-3 cells used in this experiment.

of STAT6 was markedly reduced in the presence of siRNA directed against AnxA2. These results indicate that endogenous AnxA2 upregulates the transcriptional activity of STAT6.

It has previously been shown that the transcriptional activity of the STAT family of proteins is enhanced by nonclassical activators of STAT-mediated transcription (*32*). In MCF-7 breast cancer cells, type IV collagen induces the nuclear translocation and increases the DNA binding activity of STAT5 (*52*). Furthermore, STAT6 transcriptional activity depends on its binding to coregulatory molecules like cAMP response element binding protein (CBP) and p300 (*53*, *54*). The CBP−p300 complex binds to the STAT6 transactivation domain (TAD) and the basal transcription machinery at the promoter to facilitate the transcription of STAT6 target genes (*46*). Since AnxA2 interacts with the STAT6 DNA-binding elements and facilitates STAT6-mediated transcription, further studies are necessary to prove whether AnxA2 is a nonclassical activator of STAT6 transcription.

AnxA2 is known to translocate to the nucleus and facilitate DNA replication (*55*), and our previous studies have shown that STAT6 expression protects prostate cancer cells by upregulating anti-apoptotic proteins Bcl-X_L and Bcl-2 (*29*) and activates the migratory and invasive phenotype. Thus, it is tempting to speculate that AnxA2 acts as a transcriptional coactivator of STAT6 there by transcriptionally upregulating STAT6 downstream genes, facilitating progression of the disease.

This study is the first to demonstrate the association of AnxA2 with a member of the STAT family. Although AnxA2 and STAT6 are expressed in normal cells, several studies have suggested that they are constitutively overexpressed in metastatic cancer (*12*, *25*, *30*, *56*). The downstream signaling mediators that contribute to AnxA2 and STAT6-mediated metastatic processes

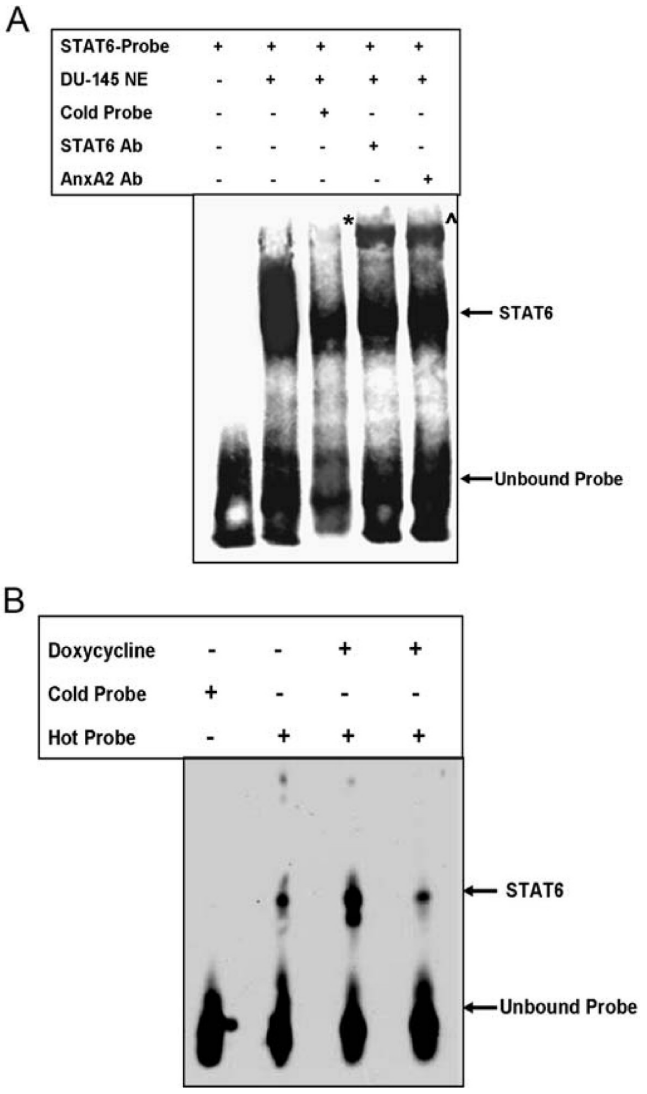

FIGURE 8: AnxA2 stimulates STAT6 DNA binding activity in prostate cancer cells. (A) Nuclear lysates from DU-145 cells were used for the EMSA. A cold probe served as a competitor for the STAT6 probe, showing the specificity of the reactions. The STAT6−DNA complex was further supershifted with STAT6 antibody (*) and the AnxA2 antibody (^), confirming the presence of the STAT6−AnxA2 complex in nuclear lysates. (B) Nuclear lysates from LNCaP stable cells expressing the doxycycline-inducible AnxA2 gene were used for the EMSA. Nuclear lysates from 2 μg/mL doxycycline-stimulated LNCaP-12 cells were incubated with the STAT6 probe (lane 3), whereas unstimulated cells incubated with either the unlabeled probe (lane 1) or the STAT6 probe served as negative controls (lane 2). The HeLa cell nuclear lysate incubated with the STAT6 probe served as a positive control reaction for the EMSA (lane 4).

have also been well established (*20*, *32*). In this report, we have identified STAT6 as a binding partner of AnxA2 in metastatic prostate cancer cells and also demonstrated that AnxA2 enhances the transcriptional activity of STAT6. Although we did not test the AnxA2−STAT6 interaction in normal cells in this study, we speculate that this interaction can be functionally significant in cancer cells overexpressing both AnxA2 and STAT6. On the basis of our results, we predict that the individual effects of STAT6 and AnxA2 in metastatic cancer progression could be potentiated by their physical interaction. Further studies are necessary to identity the downstream signaling molecules that are directly influenced by AnxA2−STAT6 interaction and subsequently contribute to metastatic cancer progression.

ACKNOWLEDGMENT

We acknowledge Dr. Jie Liu, Dr. Rafal Luchowski, Cherice Roth, and Debamita Chatterjee for assistance with different experiments.

REFERENCES

1. Gupta, G. P., and Massague, J. (2006) Cancer Metastasis: Building a Framework. *Cell 127*, 679–695.
2. Alexandrova, A. Y. (2008) Evolution of Cell Interactions with Extracellular Matrix during Carcinogenesis. *Biochemistry* (*Moscow, Russ. Fed.*) *73*, 733–741.
3. Wilson, T. J., and Singh, R. K. (2008) Proteases as Modulators of Tumor-Stromal Interaction: Primary Tumors to Bone Metastases. *Biochim. Biophys. Acta 1785*, 85–95.
4. Kwaan, H. C., and McMahon, B. (2009) The Role of Plasminogen-Plasmin System in Cancer. *Cancer Treat. Res. 148*, 43–66.
5. Dano, K., Behrendt, N., Hoyer-Hansen, G., Johnsen, M., Lund, L. R., Ploug, M., and Romer, J. (2005) Plasminogen Activation and Cancer. *Thromb. Haemostasis 93*, 676–681.
6. Hajjar, K. A., and Krishnan, S. (1999) Annexin II: A Mediator of the plasmin/plasminogen Activator System. *Trends Cardiovasc. Med. 9*, 128–138.
7. Cesarman, G. M., Guevara, C. A., and Hajjar, K. A. (1994) An Endothelial Cell Receptor for plasminogen/tissue Plasminogen Activator (t-PA). II. Annexin II-Mediated Enhancement of t-PA-Dependent Plasminogen Activation. *J. Biol. Chem. 269*, 21198–21203.
8. Rescher, U., and Gerke, V. (2004) Annexins: Unique Membrane Binding Proteins with Diverse Functions. *J. Cell Sci. 117*, 2631–2639.
9. Esposito, I., Penzel, R., Chaib-Harrireche, M., Barcena, U., Bergmann, F., Riedl, S., Kayed, H., Giese, N., Kleeff, J., Friess, H., and Schirmacher, P. (2006) Tenascin C and Annexin II Expression in the Process of Pancreatic Carcinogenesis. *J. Pathol. 208*, 673–685.
10. Mai, J., Finley, R. L., Jr., Waisman, D. M., and Sloane, B. F. (2000) Human Procathepsin B Interacts with the Annexin II Tetramer on the Surface of Tumor Cells. *J. Biol. Chem. 275*, 12806–12812.
11. Cesarman, G. M., Guevara, C. A., and Hajjar, K. A. (1994) An Endothelial Cell Receptor for plasminogen/tissue Plasminogen Activator (t-PA). II. Annexin II-Mediated Enhancement of t-PA-Dependent Plasminogen Activation. *J. Biol. Chem. 269*, 21198–21203.
12. Sharma, M. C., and Sharma, M. (2007) The Role of Annexin II in Angiogenesis and Tumor Progression: A Potential Therapeutic Target. *Curr. Pharm. Des. 13*, 3568–3575.
13. Sharma, M. R., Koltowski, L., Ownbey, R. T., Tuszynski, G. P., and Sharma, M. C. (2006) Angiogenesis-Associated Protein Annexin II in Breast Cancer: Selective Expression in Invasive Breast Cancer and Contribution to Tumor Invasion and Progression. *Exp. Mol. Pathol. 81*, 146–156.
14. Diaz, V. M., Hurtado, M., Thomson, T. M., Reventos, J., and Paciucci, R. (2004) Specific Interaction of Tissue-Type Plasminogen Activator (t-PA) with Annexin II on the Membrane of Pancreatic Cancer Cells Activates Plasminogen and Promotes Invasion in Vitro. *Gut 53*, 993–1000.
15. Yao, H., Zhang, Z., Xiao, Z., Chen, Y., Li, C., Zhang, P., Li, M., Liu, Y., Guan, Y., Yu, Y., and Chen, Z. (2009) Identification of Metastasis Associated Proteins in Human Lung Squamous Carcinoma using Two-Dimensional Difference Gel Electrophoresis and Laser Capture Microdissection. *Lung Cancer 65*, 41–48.
16. Ohno, Y., Izumi, M., Kawamura, T., Nishimura, T., Mukai, K., and Tachibana, M. (2009) Annexin II Represents Metastatic Potential in Clear-Cell Renal Cell Carcinoma. *Br. J. Cancer 101*, 287–294.
17. Duncan, R., Carpenter, B., Main, L. C., Telfer, C., and Murray, G. I. (2008) Characterisation and Protein Expression Profiling of Annexins in Colorectal Cancer. *Br. J. Cancer 98*, 426–433.
18. Emoto, K., Sawada, H., Yamada, Y., Fujimoto, H., Takahama, Y., Ueno, M., Takayama, T., Uchida, H., Kamada, K., Naito, A., Hirao, S., and Nakajima, Y. (2001) Annexin II Overexpression is Correlated with Poor Prognosis in Human Gastric Carcinoma. *Anticancer Res. 21*, 1339–1345.
19. Shiozawa, Y., Havens, A. M., Jung, Y., Ziegler, A. M., Pedersen, E. A., Wang, J., Wang, J., Lu, G., Roodman, G. D., Loberg, R. D., Pienta, K. J., and Taichman, R. S. (2008) Annexin II/annexin II Receptor Axis Regulates Adhesion, Migration, Homing, and Growth of Prostate Cancer. *J. Cell. Biochem. 105*, 370–380.
20. Inokuchi, J., Narula, N., Yee, D. S., Skarecky, D. W., Lau, A., Ornstein, D. K., and Tyson, D. R. (2009) Annexin A2 Positively Contributes to the Malignant Phenotype and Secretion of IL-6 in DU145 Prostate Cancer Cells. *Int. J. Cancer 124*, 68–74.
21. Yee, D. S., Narula, N., Ramzy, I., Boker, J., Ahlering, T. E., Skarecky, D. W., and Ornstein, D. K. (2007) Reduced Annexin II Protein Expression in High-Grade Prostatic Intraepithelial Neoplasia and Prostate Cancer. *Arch. Pathol. Lab. Med. 131*, 902–908.
22. Banerjee, A. G., Liu, J., Yuan, Y., Gopalakrishnan, V. K., Johansson, S. L., Dinda, A. K., Gupta, N. P., Trevino, L., and Vishwanatha, J. K. (2003) Expression of Biomarkers Modulating Prostate Cancer Angiogenesis: Differential Expression of Annexin II in Prostate Carcinomas from India and USA. *Mol. Cancer 2*, 34.
23. Liu, J. W., Shen, J. J., Tanzillo-Swarts, A., Bhatia, B., Maldonado, C. M., Person, M. D., Lau, S. S., and Tang, D. G. (2003) Annexin II Expression is Reduced Or Lost in Prostate Cancer Cells and its Re-Expression Inhibits Prostate Cancer Cell Migration. *Oncogene 22*, 1475–1485.
24. Takeda, K., and Akira, S. (2000) STAT Family of Transcription Factors in Cytokine-Mediated Biological Responses. *Cytokine Growth Factor Rev. 11*, 199–207.
25. Konjevic, G. (2009) STAT Proteins in Cancerogenesis and Therapy of Malignancies. *Srp. Arh. Celok. Lek. 137*, 98–105.
26. Wang, L., Yi, T., Kortylewski, M., Pardoll, D. M., Zeng, D., and Yu, H. (2009) IL-17 can Promote Tumor Growth through an IL-6-Stat3 Signaling Pathway. *J. Exp. Med. 206*, 1457–1464.
27. Takemoto, S., Ushijima, K., Kawano, K., Yamaguchi, T., Terada, A., Fujiyoshi, N., Nishio, S., Tsuda, N., Ijichi, M., Kakuma, T., Kage, M., Hori, D., and Kamura, T. (2009) Expression of Activated Signal Transducer and Activator of Transcription-3 Predicts Poor Prognosis in Cervical Squamous-Cell Carcinoma. *Br. J. Cancer 101*, 967–972.
28. Bernaciak, T. M., Zareno, J., Parsons, J. T., and Silva, C. M. (2009) A Novel Role for Signal Transducer and Activator of Transcription 5b (STAT5b) in β1-Integrin-Mediated Human Breast Cancer Cell Migration. *Breast Cancer Res. 11*, R52.
29. Das, S., Roth, C. P., Wasson, L. M., and Vishwanatha, J. K. (2007) Signal Transducer and Activator of Transcription-6 (STAT6) is a Constitutively Expressed Survival Factor in Human Prostate Cancer. *Prostate 67*, 1550–1564.
30. Li, B. H., Yang, X. Z., Li, P. D., Yuan, Q., Liu, X. H., Yuan, J., and Zhang, W. J. (2008) IL-4/Stat6 Activities Correlate with Apoptosis and Metastasis in Colon Cancer Cells. *Biochem. Biophys. Res. Commun. 369*, 554–560.
31. Bromberg, J. (2002) Stat Proteins and Oncogenesis. *J. Clin. Invest. 109*, 1139–1142.
32. Hebenstreit, D., Wirnsberger, G., Horejs-Hoeck, J., and Duschl, A. (2006) Signaling Mechanisms, Interaction Partners, and Target Genes of STAT6. *Cytokine Growth Factor Rev. 17*, 173–188.
33. Zhang, W. J., Li, B. H., Yang, X. Z., Li, P. D., Yuan, Q., Liu, X. H., Xu, S. B., Zhang, Y., Yuan, J., Gerhard, G. S., Masker, K. K., Dong, C., Koltun, W. A., and Chorney, M. J. (2008) IL-4-Induced Stat6 Activities Affect Apoptosis and Gene Expression in Breast Cancer Cells. *Cytokine 42*, 39–47.
34. Jensen, S. M., Meijer, S. L., Kurt, R. A., Urba, W. J., Hu, H. M., and Fox, B. A. (2003) Regression of a Mammary Adenocarcinoma in STAT6$^{-/-}$ Mice is Dependent on the Presence of STAT6-Reactive T Cells. *J. Immunol. 170*, 2014–2021.
35. Sasaki, K., Zhao, X., Pardee, A. D., Ueda, R., Fujita, M., Sehra, S., Kaplan, M. H., Kane, L. P., Okada, H., and Storkus, W. J. (2008) Stat6 Signaling Suppresses VLA-4 Expression by CD8+ T Cells and Limits their Ability to Infiltrate Tumor Lesions in Vivo. *J. Immunol. 181*, 104–108.
36. Lee, S. O., Pinder, E., Chun, J. Y., Lou, W., Sun, M., and Gao, A. C. (2008) Interleukin-4 Stimulates Androgen-Independent Growth in LNCaP Human Prostate Cancer Cells. *Prostate 68*, 85–91.
37. Liu, J., Rothermund, C. A., Ayala-Sanmartin, J., and Vishwanatha, J. K. (2003) Nuclear Annexin II Negatively Regulates Growth of LNCaP Cells and Substitution of Ser 11 and 25 to Glu Prevents Nucleo-Cytoplasmic Shuttling of Annexin II. *BMC Biochem. 4*, 10.
38. Tatenhorst, L., Rescher, U., Gerke, V., and Paulus, W. (2006) Knockdown of Annexin 2 Decreases Migration of Human Glioma Cells in Vitro. *Neuropathol. Appl. Neurobiol. 32*, 271–277.
39. Wallrabe, H., and Periasamy, A. (2005) Imaging Protein Molecules using FRET and FLIM Microscopy. *Curr. Opin. Biotechnol. 16*, 19–27.
40. Lakowicz, J. R. (1983) Priniciples of Fluorescence Spectroscopy, 3rd ed., Plenum, New York.
41. Huuskonen, J., Vishnu, M., Pullinger, C. R., Fielding, P. E., and Fielding, C. J. (2004) Regulation of ATP-Binding Cassette Transporter A1 Transcription by Thyroid Hormone Receptor. *Biochemistry 43*, 1626–1632.

42. Dasgupta, S., Wasson, L. M., Rauniyar, N., Prokai, L., Borejdo, J., and Vishwanatha, J. K. (2009) Novel Gene C17orf37 in 17q12 Amplicon Promotes Migration and Invasion of Prostate Cancer Cells. *Oncogene 28*, 2860–2872.
43. Mikita, T., Campbell, D., Wu, P., Williamson, K., and Schindler, U. (1996) Requirements for Interleukin-4-Induced Gene Expression and Functional Characterization of Stat6. *Mol. Cell. Biol. 16*, 5811–5820.
44. Baran, D. T., Quail, J. M., Ray, R., and Honeyman, T. (2000) Binding of 1α,25-Dihydroxyvitamin D_3 to Annexin II: Effect of Vitamin D Metabolites and Calcium. *J. Cell. Biochem. 80*, 259–265.
45. Kassam, G., Manro, A., Braat, C. E., Louie, P., Fitzpatrick, S. L., and Waisman, D. M. (1997) Characterization of the Heparin Binding Properties of Annexin II Tetramer. *J. Biol. Chem. 272*, 15093–15100.
46. McDonald, C., and Reich, N. C. (1999) Cooperation of the Transcriptional Coactivators CBP and p300 with Stat6. *J. Interferon Cytokine Res. 19*, 711–722.
47. Calo, V., Migliavacca, M., Bazan, V., Macaluso, M., Buscemi, M., Gebbia, N., and Russo, A. (2003) STAT Proteins: From Normal Control of Cellular Events to Tumorigenesis. *J. Cell. Physiol. 197*, 157–168.
48. Takeda, K., and Akira, S. (2000) STAT Family of Transcription Factors in Cytokine-Mediated Biological Responses. *Cytokine Growth Factor Rev. 11*, 199–207.
49. Zimmermann, U., Woenckhaus, C., Pietschmann, S., Junker, H., Maile, S., Schultz, K., Protzel, C., and Giebel, J. (2004) Expression of Annexin II in Conventional Renal Cell Carcinoma is Correlated with Fuhrman Grade and Clinical Outcome. *Virchows Arch. 445*, 368–374.
50. Hoey, T., and Schindler, U. (1998) STAT Structure and Function in Signaling. *Curr. Opin. Genet. Dev. 8*, 582–587.
51. Daines, M. O., Andrews, R. P., Chen, W., El-Zayaty, S. A., and Hershey, G. K. (2003) DNA Binding Activity of Cytoplasmic Phosphorylated Stat6 is Masked by an Interaction with a Detergent-Sensitive Factor. *J. Biol. Chem. 278*, 30971–30974.
52. Robledo, T., Arriaga-Pizano, L., Lopez-Perez, M., and Salazar, E. P. (2005) Type IV Collagen Induces STAT5 Activation in MCF7 Human Breast Cancer Cells. *Matrix Biol. 24*, 469–477.
53. Valineva, T., Yang, J., Palovuori, R., and Silvennoinen, O. (2005) The Transcriptional Co-Activator Protein p100 Recruits Histone Acetyltransferase Activity to STAT6 and Mediates Interaction between the CREB-Binding Protein and STAT6. *J. Biol. Chem. 280*, 14989–14996.
54. Shankaranarayanan, P., Chaitidis, P., Kuhn, H., and Nigam, S. (2001) Acetylation by Histone Acetyltransferase CREB-Binding protein/p300 of STAT6 is Required for Transcriptional Activation of the 15-Lipoxygenase-1 Gene. *J. Biol. Chem. 276*, 42753–42760.
55. Vishwanatha, J. K., and Kumble, S. (1993) Involvement of Annexin II in DNA Replication: Evidence from Cell-Free Extracts of Xenopus Eggs. *J. Cell Sci. 105* (Part 2), 533–540.
56. Mohammad, H. S., Kurokohchi, K., Yoneyama, H., Tokuda, M., Morishita, A., Jian, G., Shi, L., Murota, M., Tani, J., Kato, K., Miyoshi, H., Deguchi, A., Himoto, T., Usuki, H., Wakabayashi, H., Izuishi, K., Suzuki, Y., Iwama, H., Deguchi, K., Uchida, N., Sabet, E. A., Arafa, U. A., Hassan, A. T., El-Sayed, A. A., and Masaki, T. (2008) Annexin A2 Expression and Phosphorylation are Up-Regulated in Hepatocellular Carcinoma. *Int. J. Oncol. 33*, 1157–1163.